Journal of Medicinal and Nanomaterials Chemistry 2 (2021) 125-134

Journal of Medicinal and Nanomaterials Chemistry

Journal homepage: https://jmnc.samipubco.com/

Orginal Research Article

Reduced graphene oxide/nanohydroxy Apatite-Bismuth nanocomposites for osteogenic differentiation of human mesenchymal stem cells

Seyedeh Mahsa Khatami[a], Shadie Hatamie[b,*], Alireza Naderi Sohi[c], Kazem Parivar[a], Masoud Soliemani[d], Hana Hanaee-Ahvaz[c,*]

[a] *Department of Biology, Science and Research Branch, Islamic Azad University, Tehran, Iran*

[b] *College of Medicine, National Taiwan University, 10048, Taipei, Taiwan*

[c] *Stem Cell Technology Research Center, Tehran, Iran*

[d] *Department of Hematology, Faculty of Medical Sciences, Tarbiat Modares University, Tehran, Iran*

ARTICLE INFORMATION

Received: 5 October 2020
Received in revised: 12 January 2021
Accepted: 13 February 2021
Available online: 16 February 2021

DOI: 10.48309/JMNC.2021.2.4

KEYWORDS

Graphene
Bismuth
Nano-hydroxyapatite
Adipose derived stem cells

ABSTRACT

Graphene/hydroxyapatite nanocomposites (NCs) is attracted more attention in bone tissue engineering due to their osteoconductive properties. Adding different ionic substitutions to graphene/hydroxyapatite NCs may increase its osteogenic properties. In this research study, bismuth doped hydroxyapatite nano-rods (Bi-nHA) were decorated on the reduced graphene oxide (rGO) sheets. The formation and structure of the nanocomposites (rGO/Bi-nHA) was characterized using the transmission electron microscope (TEM), X-ray diffraction (XRD), Fourier transform infrared spectroscopy (FTIR), Raman spectroscopy, Inductively-coupled plasma optical emission spectroscopy (ICP-OES), and zeta potential. The characterization results revealed that the graphene is reduced and the nanocomposites are multilayer. Zeta potential of nanocomposite sheets is seen to be-23.1 mV. The cytotoxicity and osteoconductive effects of rGO/Bi-nHA nanocomposite on Human adipose derived stem cells (ADSCs) were examined using the MTT and calcium deposition assay. The results demonstrated that, the nanocomposites have no toxicity. Calcium deposition was observed at all concentrations and the highest calcium deposition is at 10 µg/mL. Based on the results of the synthesized nanocomposites, this material is suitable to be utilized in scaffold construction for bone tissue engineering.

Corresponding authors, email: shadyhatamy@gmail.com(S. Hatamie).
Tel.: +00886966230784.

Graphical Abstract

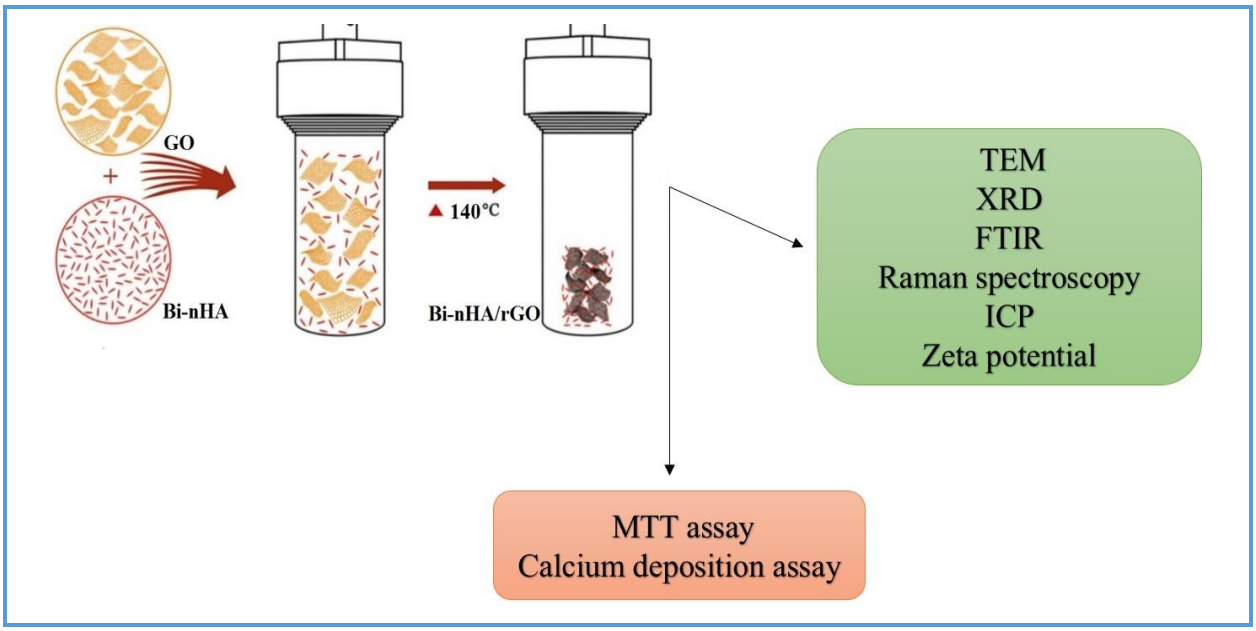

Introduction

Molecular behavior at the nanometer scale manages living systems. Nanotechnology is the ability to make, control and use matter in nanometer dimensions. Particle size is very important in nanotechnology, because at a nano scale, the dimensions of matter are very influential in its properties, and the physical, chemical, and biological properties. Nanotechnology is a wide range of applications of nanomaterials such as nanoparticles [1–3] and nanocomposites for environmental contamination remove [4–7], medical and industrial affairs to design of biosensors, drug delivery and tissue engineering [8].

Nanocomposites are a group of hybrid materials made from biodegradable synthetic or natural polymers, organic and inorganic materials. One of the various features of the nanocomposites is the high surface to volume ratio, flexibility without reducing its strength. The different chemical structures of these materials make them more applicable in tissue engineering and weight-bearing composites in bone regeneration. An important and influential factor in the biomedical properties of the nanocomposites is the interaction in the matrix [9]. Study of nanomaterial has been considered by many researchers due to their relevance to the human health [10, 11].

Nanomaterials have been used in wide range of tissue engineering studies especially in bone tissue engineering. There are several types of materials which are used in bone repair such as metals, ceramics, hard polymers and their composites. Over the last two decades, calcium phosphate derivatives such as hydroxyapatite (HA, $Ca_{10}(PO_4)_6(OH)_2$), widely used in bone repair applications due to its unique properties such as biocompatibility, bioactivity and osteoconductivity [12, 13]. HA has a bone-like structure which can effectively promote the osteoblast growth and could stimulate mineralization of osteoid [14]. The only drawback is its poor mechanical properties and inherent fragility, which encouraged many researchers to concentrate on improving HA mechanical properties by adding novel elements to make its composites [15–18]. Nano-

HA has several structural and morphological like, nanorods, nanotubes and nanosphere, with different mechanical impact [19]. However other modifications are still required further improvement the mechanical characteristics of nano HA. HA is synthetized using various methods such as hydrothermal, microwave and precipitation methods [24], [25] and is created in spherical, rod like, fiber like and flower like shapes [26]. Nano-HA can be doped with metals such as as silver, and iron [27] to grant novel properties including, magnetic and antimicrobial activity. Bismuth is a chemical element that has been used in many pharmaceuticals as an anti-diarrheal and anti-bacterial agent [28] [29]. Webster *et al*, [20] doped hydroxyapatite (HA) with various metal cations such as Mg^{2+}, Zn^{2+} and Bi^{3+} in an attempt to enhance properties of HA pertinent to orthopedic and dental applications. Accordingly, Bi^{3+} highly enhanced osteoblasts for long-term calcium deposition [30].

Carbon nano-materials have been used as fillers in ceramic matrices to make composites, due to their excellent mechanical properties including, Young's modulus (up to 1 TPa) and intrinsic strength (approximately 130 GPa) [21, 22]. Graphene is a single-atom-thick sheet with sp^2-bonded carbon atoms in a closely packed two dimensional (2D) honeycomb crystal with large surface area ~2600 $m^2.g^{-1}$ [23]. Graphene sheets have extremely high electrical and thermal conductivity [24] and mechanical strength [25]. Graphene-sheets are available in mono- or multilayered graphene layers [26] or chemical modification [27]. This materials are hydrophilic and could functionalize biochemically [28]. Also, graphene indicates low cost and inherent biocompatibility [29]. Recent studies have showed that graphene has a osteogenic potential to promote the osteoblast differentiation [30]. Chaudhuri *et al*. [35] demonstrated that the graphene might be used as potential candidates for mesenchymal stem cells differentiation and proliferation for human skeletal muscle tissue regeneration [31]. Different graphene-based composites have been synthetized for bone tissue engineering. These properties have generated a great deal of interest in the scientific community. In this study, the rGO/Bi-nHA nanocomposites were synthesized using the hydrothermal process and the biocompatibility and osteoconductivity of the nanocomposite was studied using the human adipose derived stem cells (ADSCs).

Materials and Methods

Materials

Graphite powder (mesh ≤200µm), potassium permanganate ($KMnO_4$), sulfuric acid (H_2SO_4), sodium nitrate ($NaNO_3$), hydrogen peroxide (H_2O_2), calcium nitrate ($Ca(NO_3)_2$), bismuth nitrate ($Bi(NO_3)_2$), di-Ammonium hydrogen phosphate $NaH_2(PO_4)_2$, of Merck were used in the chemical fabrication process, without further purification. DMEM, FBS, dexamethasone, β-glycerol phosphate, ascorbic acid bisphosphate of sigma as well as abdominal adipose tissue were used in cellular part.

Methods

Preparation of Graphene Oxide (GO)

Graphene oxide (GO) was prepared using the modified Hummers' method [32]. Graphite powder (0.5 g) and sodium nitrate (0.5 g) were dissolved in 23 mL of sulfuric acid in ice bath. Then, the $KMnO_4$ (3 g) was added to the mixture and the temperature was increased to 35 °C. The mixture was stirred under the same temperature for 4 h. After completing the reaction, deionized water (40 mL) was added drop-wise to the solution. Finally, in the end of

process, deionized water (100 mL) and H_2O_2 (3 mL) were added to the solution. The mixture color changes bright yellow, as graphite oxide get formed. The graphite oxide suspension is filtered and washed with HCl and deionized water followed by wash with deionized water till tune the pH at 5. The graphite oxide solution was ultra-sonicated (100 W, 20 kHz) for 1h to get exfoliated to the GO sheets.

Synthesis of Bi Doped Hydroxyapatite Nanorod (Bi-nHA)

$Ca(NO_3)_2.4H_2O$ (1.18 g) was dissolved in 5 mL double distilled water. Then the $(NH_4)_2HPO_4$ and Bi $(NO_3).5H_2O$ were dissolved in aqueous media using ultra-sonication. Then $Bi(NO_3).5H_2O$ aqueous solution was added dropwise to $Ca(NO_3)_2.4H_2O$ solution. The mixture was stirred for 1 h at 40 °C. Finally, the $(NH_4)_2HPO_4$ solution was added drop wise to the mixture. pH of sample is adjusted to 10 in each step using ammonium solution. The mixture was stirred for 4 h at 40 °C. The resultant material was centrifuged (10 min, 2500 rpm) in aqueous media till the pH become 7. The precipitate was dried at room temperature.

Synthesis of rGO/Bi-nHA nano Composites

To prepare nano composites, 0.1 g GO was dissolved in 40 mL distilled water. Besides, 0.1 g Bi-nHA was added to the GO solution and pH was adjusted to 11 using ammonia solution. The rGO/Bi-nHA mixture was poured in stainless steel Teflon lined autoclaved and was incubated at 140 ^oC in oven for 5 h. After time passes, mixture was centrifuged (15 min, 3000 rpm) till the pH become 7. The precipitate was dried for 48 h at 50 °C in an oven.

Characterization of rGO/Bi-nHA Nanocomposites

The nanocomposites morphology and sizes were investigated using the transmission electron microscopy (TEM, JEOL JEM-2010). The XRD patterns were obtained using a Philips X'Pert Pro MRD system (λ=1.54 Å) and FTIR spectrums were gained by using an Equinox 55, Bruker. Raman spectroscopy was performed using HR-800 Jobin-Yvon system with Nd-YAG laser source operating at wavelength of 532 nm at room temperature. Zeta potential was performed to measure the electrical charge of nanocomposite using Malvern Instrument Ltd-UK. The rGO/Bi-nHA nano composites loading percentage was confirmed using inductively coupled plasma optical emission spectrometry (ICP-OES) using the Spectro Arcos instrument.

hADSCs Isolation and Characterization

hADSCs isolation was performed according to Pakfar *et al.* [33]. The liposuction sample was washed several times with normal saline. At the next step, collagenase IV was added and the sample was incubated for 45 min at 37 °C while on shaker at 250 rpm. Collagenase was removed by centrifugation at 1200 rpm for 10 min. The pellet was then incubated with RBC lysis buffer to remove blood cells. The cells were cultured in DMEM supplemented with 10% FBS, 1% pen/strep and 1% amphotericin (all from sigma) in incubator (5% CO2 at 37 °C). Cells which were used in differentiation experiments were in passages 3 to 6 [33].

Viability Test

To evaluate the nanocomposites cytotoxicity, the ADSCs (typically $\sim 3\times10^3$ cells) were cultured in DMEM F12, supplemented with 10% FBS and 1% penstrep at 37 °C under 5% CO_2. ADSCs were treated with 1, 3, 5, 7 and 10 µg/mL of rGO/Bi-nHA nano-composites. The medium was removed after culture for 1, 3, 5 and 7 days and cell viability

were checked using the MTT assay. The optical density (OD) was measured at 570 nm using the Bio-Tek ELX8000 microplate reader.

Calcium deposition measurements

To detect the mineralization and calcium deposition of the ADSCs (2×10^4 cells), cells were cultured in DMED F12, supplemented with 10% FBS and 1% pen strep. The cells were treated with rGO/Bi-nHA nanocomposites in 1, 3, 5, 7 and 10 µg/mL and osteogenic medium (OM) for 14 days. Standard osteogenic differentiation medium consists of ascorbic acid, Dexamethasone (10^{-7} M) and β-glycero phosphate (10^{-2} M) and DMEM F12. After 14 days, the medium was removed and the cells washed with PBS. The calcium content was extracted by HCl and measured using the calcium detection Kit (Pars azmoon, Iran) according to the manufacturer instruction. Finally, optical density was measured at 570 nm using Bio-Tek ELX8000 microplate reader at 570 nm. All data normalized against total protein using BCA kit.

Statistical Analysis

One-way analysis of variance (ANOVA) was used to compare results. Data were presented as average ±SD. Data were reported as significant if $P<0.05$.

Results and Discussion

Characterization of rGO/Bi-nHA Nanocomposites

Figure 1 demonstrates the TEM images of the rGO/Bi-nHA nanocomposites. As seen in Figure 1, the Bi-nHA nano rods are attached on the rGO surfaces. The rGO sheets are stick to each other to made two and/or three layers. The average size of the graphene sheets are around 2 µm and the length of the Bi-nHA nanowire are seen to be 200 nm with the diameter of around 50 nm.

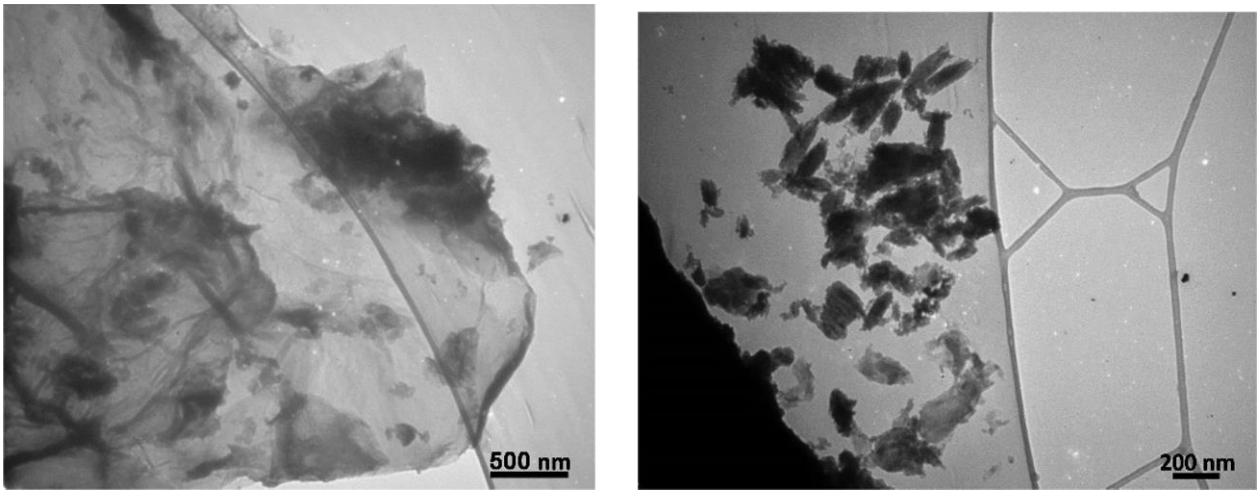

Figure 1. TEM images of rGO/Bi-nHA nanocomposites

The XRD technique (Figure 2a), was used to confirm the structure of rGO/Bi-nHA nanocomposites. The characteristic peaks of nHA was placed at 2θ~24.97, 30.84, corresponding to the (002), (211) planes respectively. Bismuth characteristic peaks was detected at 2θ~27.26,40,48 corresponding to the (012), (110), (202) planes of it. The characteristic peaks of the GO materials which should appear at 2θ~11° were vanished, it

means that the GO are reduced through the synthesized. Reduction of GO and doping of Bi with nHA were checked using FT-IR (Figure 2b). The absorbance band at 3428 cm^{-1} is assigned to the hydroxyl group (-OH) stretching bond. The 1655 and 1573 cm^{-1} bands is related to ($C=C$) in rGO. The P=O band of nHA was seen at 1109, 1022 and 558.468 cm^{-1}, respectively. The vibration band of –OH is located at 795.668 cm^{-1}. Finally, the 594.69 cm^{-1} band indicates Bi-O and bismuth doping on nHA.

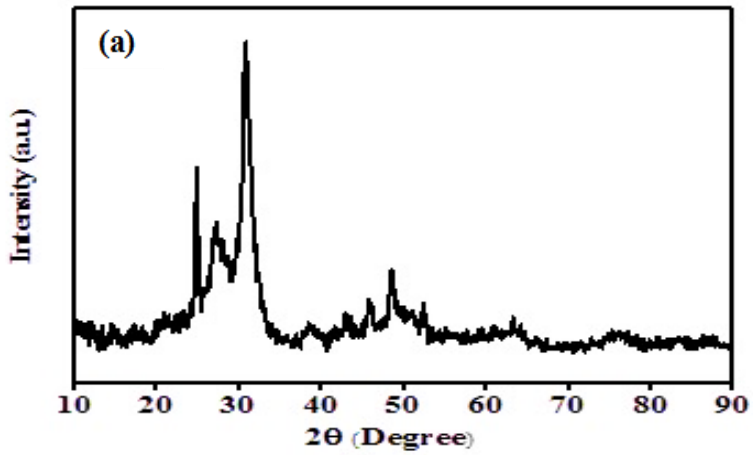

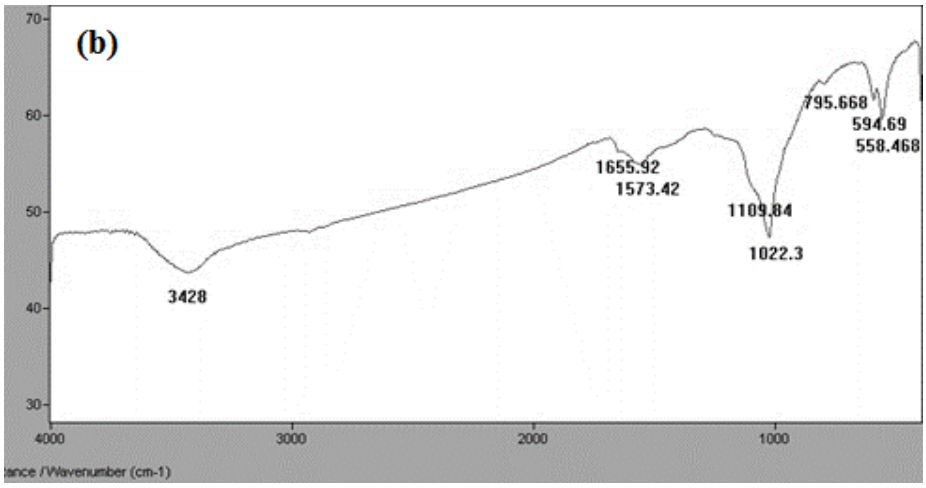

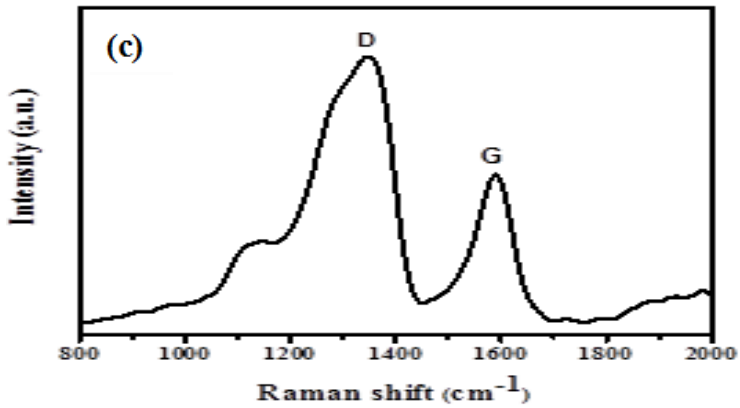

Figure 2. a) XRD, b) FT-IR and c) Raman spectroscopy of the rGO/Bi-nHA nanocomposites

Figure 2c, displays the Raman spectra of the rGO/Bi-nHA nanocomposites. As seen in Figure 2, the peaks of D and G bonds of graphitic materials are placed at 1349, 1592 cm^{-1} respectively. The G peaks position is shifted to higher wave lengths which could be corresponding to the doping impurities in graphene. The I_D/I_G are calculated to be 1.78, which is increased compared to the 1.16 of GO, which is confirmed the reduction of the GO and diminished the oxygen functionalized groups. Furthermore, the I_{2D}/I_G ratio of the rGO/Bi-nHA was found 0.28. These results indicated in the rGO/Bi-nHA nanocomposites graphene is multilayer.

The ion-coupled plasma optical emission spectroscopy (ICP-OES) was used to find the atomic concentration of elements (Ca and Bi) in the rGO/Bi-nHA nanocomposites. The amount of Ca and Bi are reported to be 9.12 and 21.6 weight percent (wt %), respectively in nanocomposites which means the maximum amount of is for the reduced graphene oxide. These results showed that the graphene materials occupied approximate 69.28 wt% of the nanocomposites. As the cell membranes have usually charge, the surface charge of nanomaterials play a key role in cell-nanomaterial interactions [34]. Zeta potentials of the rGO/Bi-nHA is equal to -23.1 mV, which is increased compared to the GO which is -40 mV, because of the decoration of the graphene surfaces by Bi-nHA.

MTT assay

The MTT assay was designed to probe the activity of reductase enzymes as a measure of cell viability and proliferation. Figure 3 represents the viability of the cells when treated with different concentrations of rGO/Bi-nHA for 1, 3, 5 and 7 days. Human ADSCs show different biological responses, when exposed to different treatment duration and dosage of rGO/Bi-nHA nanocomposites. At all concentrations, there is an increasing trend from days 1 to day 7. At lower nanocomposites concentrations (1, 3 and 5 µg/mL) cells showed somehow similar proliferation rate as that of control group. Treatment with higher concentration of nanocomposites led to lower cell proliferation rates. However, it can be concluded that at concentrations of 7 and 10 µg / ml the cells have more than 50% viability.

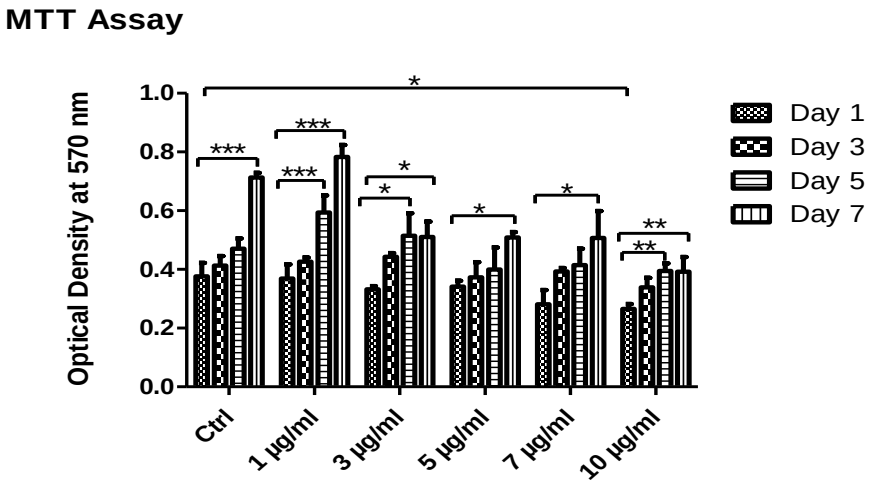

Figure 3. MTT assay after 1, 3, 5 and 7 days showing the rate of ADSCs viability in presence of rGO/Bi-nHA nanocomposites (*p value < 0.05, ** p value < 0. 01 and ***p < 0.001)

Calcium assay

The calcium assay represents the amount of Ca deposition by ADSCs and can be considered as a marker of osteogenic differentiation. Human ADSCs was treated by 1, 3, 5, 7 and 10 µg/mL rGO/Bi-nHA and osteogenic medium (OM) for 14 days. Calcium deposition was observed at all concentrations. Concentrations of 1–7 µg/mL showed similar calcium deposition to the osteogenic medium, whereas 10 µg/mL revealed a significant increase in calcium deposition compared to lower concentrations in the osteogenic medium. Various studies have been performed to investigate the viability of different cells such as osteoblasts [9] and osteoblast-like cells [35] on derivatives of graphene and hydroxyapatite [30]. Some studies showed that the graphene, graphene/hydroxyapatite derivatives are biocompatible. Studies on various types of doping ions on hydroxyapatite and graphene oxide have also shown their biocompatibility [20, 36]. The proliferation rate in the low concentration groups was similar to the control group. Proliferation of 10 and 7 µg/mL concentrations showed slower trend compared to the other groups. Therefore, when nanocomposites are in direct contact with mesenchymal cells, a high percentage of cultured cells remain active metabolically (above 50% at the highest concentration), indicating the biocompatibility of the synthesized nanocomposites material.

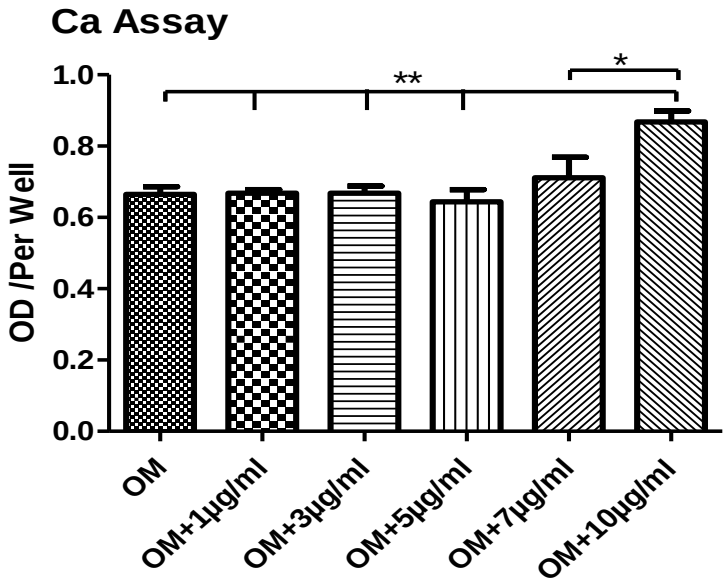

Figure 4. Evaluation of calcium deposition in the presence of rGO/Bi-nHA nanocomposites on day 14. (* $P < 0.05$)، (** $P < 0.01$)

The growth factors and inducers which are promoting osteogenic differentiation are complex and expensive. Graphene/hydroxyapatite nanocomposites have osteo-conductive potential and various studies have shown that use of these derivatives helps to strengthen its mechanical strength. Hydroxyapatite provides a synthetic surface for

trapping the osteoblast cells so that minerals containing calcium can precipitate. Also, application of the trivalent cations such as Bi^{3+}, could improve the osteogenic properties of these nanocomposites [20, 37]. In this study, 1–7 µg/mL concentration showed similar calcium deposition. However, at the 10 µg/mL concentration the highest Ca^{2+} deposition was observed compared to the lower concentrations and the control group. Therefore, it can be concluded that the presence of nanocomposites has a synergistic effect on the rate of calcium deposition by ADSCs along with osteogenic medium (Figure 4). Considering both MTT and calcium content results, the lower proliferation rate of the cells treated with 10 µg/mL nanocomposites could be attributed to the occurrence of ultimate osteogenic differentiation at shorter times.

Conclusions

This work showed that the graphene-based materials have positive effects on osteogenic differentiation. rGO/Bi-nHA nanocomposites were synthesized in situ using a hydrothermal method. Compared to the pristine nHA and GO sheets, the composites showed improvement in biological and mechanical properties. The cell culture and viability results indicated that the addition of the nanocomposites promote cells proliferation especially at lower concentrations (1 to 5 µg/mL). Therefore, Ca^{2+} deposition, results showed that the synthesized nanocomposite can help in osteogenic differentiation in 7 to 10 µg/mL. Finally, it can be concluded that rGO/Bi-nHA nanocomposites can be used in scaffold construction for orthopedic and bone tissue engineering.

Disclosure Statement

No potential conflict of interest was reported by the authors.

Research involving human participants and/or animals

This research is not involving Human Participants and/or Animals

References

[1]. Ullah N., Ansir R., Muhammad W., Jabeen S. *Asian Journal of Green Chemistry,* 2020, **4**:340
[2]. Fardood ST., Forootan R., Moradnia F., Afshari Z., Ramazani A. *Materials Research Express*, 2020, **7**:015086
[3]. Taghavi Fardood S., Moradnia F., Ramazani A. *Nanochemistry Research*, 2019, **4**:86
[4]. Moradnia F., Fardood S.T., Ramazani A., Gupta VK. *Journal of Photochemistry and Photobiology A: Chemistry*, 2020, **392**:112433
[5]. Fardood S.T., Moradnia F., Ramazani A. *Micro & Nano Letters*, 2019, **14**:986
[6]. Taghavi Fardood S., Ramazani A., Azimzadeh Asiabi P., Bigdeli Fard Y., Ebadzadeha B. *Asian Journal of Green Chemistry*, 2017, **1**:34
[7]. Singh P., Banik R.M. *Plant Science Today*, 2019, **6**:583
[8]. Moradnia F. et al., *Materials Research Express*, 2019, **6**:075057
[9]. Ajayan P.M., Schadler L.S., Braun P.V. *Nanocomposite science and technology*., 2006: John Wiley & Sons.
[10]. Moussy F. *Journal of Biomedical Materials Research Part A*., 2010, **94**:1001
[11]. Fardood S.T., Ramazani A., Joo S.W. *Journal of Applied Chemical Research*, 2017, **11**:8
[12]. Zhu J., Wong H.M., Yeung K.W.K., Tjong S.C. *Advanced Engineering Materials*, 2011, **13**:336
[13]. Kosma V., Tsoufis T., Koliou T., Kazantzis A., Beltsios K., De Hosson JTM., Gournis D. *Materials Science and Engineering: B*, 2013, **178**:457
[14]. Kim S., Ku S.H., Lim S.Y., Kim J.H., Park C.B. *Advanced Materials*, 2011, **23**:2009

[15]. Chen F., Zhu Y.J., Wang K.W., Zhao K.L. *CrystEngComm*, 2011, **13**:1858
[16]. Liu Y., Huang J., Li H. *Journal of Materials Chemistry B*, 2013, **1**:1826
[17]. Chandanshive B.B., Rai P., Rossi A.L., Ersen O., Khushalani D. *Materials Science and Engineering: C*, 2013, **33**:2981
[18]. Nathanael A.J., Mangalaraj D., Hong S.I., Masuda Y. *Materials Characterization*, 2011, **62**:1109
[19]. Baradaran S., Moghaddam E., Basirun WJ., Mehrali M., Sookhakian M., Hamdi M., Moghaddam M.R., Alias Y. *Carbon*, 2014, **69**:32
[20]. Webster T.J., Massa-Schlueter E.A., Smith J.L., Slamovich E.B. *Biomaterials*, 2004, **25**:2111
[21]. Zhang Y., Pan C. *Diamond and related materials*, 2012, **24**:1
[22]. Suk J.W., Piner R.D., An J., Ruoff R.S. *ACS nano*, 2010, **4**:6564
[23]. Zhang L., Zhang F., Yang X., Long G., Wu Y., Zhang T., Leng K., Huang Y., Ma Y. Scientific Reports, 2013, **3**:1408
[24]. Balandin A.A., Ghosh S., Bao W., Calizo I., Teweldebrhan D., Miao F., Lau CN. *Nano l Letters*, 2008, **8**:902
[25]. Geim A.K., *Science*, 2009, **324**: 1530
[26]. Ferrari A.C., Meyer J.C., Scardaci V., Casiraghi C., Lazzeri M., Mauri F., Piscanec S., Jiang D., Novoselov K.S., Roth S. *Physical review letters*, 2006, **97**:187401
[27]. Dubey N., Bentini R., Islam I., Cao T., Castro Neto A.H., Rosa V. *Stem cells international*, 2015, **2015**.
[28]. Wang G., Shen X., Wang B., Yao J., Park J. *Carbon*, 2009, **47**:1359
[29]. Du J., Cheng H.M., *Macromolecular Chemistry and Physics*, 2012, **213**: 1060
[30]. Akhavan O., Ghaderi E., Shahsavar M. *Carbon*, 2013, **59**:200
[31]. Chaudhuri B. *Biofabrication*, 2015, **7**:015009
[32]. Hummers Jr W.S., Offeman R.E. *Journal of the American Chemical Society*, 1958, **80**:1339
[33]. Pakfar A., Irani S., Hanaee-Ahvaz H. *Tissue and Cell*, 2017, **49**:122
[34]. Arvizo R.R., Miranda O.R., Thompson M.A., Pabelick C.M., Bhattacharya R., Robertson J.D., Rotello V.M., Prakash Y.S., Mukherjee P. *Nano letters*, 2010, **10**:2543
[35]. Selvakumar M., Srivastava P., Pawar HS., Francis N.K., Das B., Sathishkumar G., Subramanian B., Jaganathan S.K., George G., Anandhan S. *ACS Applied Materials & Interfaces*, 2016, **8**:4086
[36]. Pazarçeviren A.E., Tahmasebifar A., Tezcaner A., Keskin D., Evis Z. *Ceramics International*, 2018, **44**:3791
[37]. Gu M., Liu Y., Chen T., Du F., Zhao X., Xiong C., Zhou Y. *Tissue Engineering Part B: Reviews*, 2014, **20**:477

How to cite this manuscript: Seyedeh Mahsa Khatami, Shadie Hatamie*, Alireza Naderi Sohi, Kazem Parivar, Masoud Soliemani, Hana Hanaee-Ahvaz*. Reduced graphene oxide/nanohydroxy Apatite-Bismuth nanocomposites for osteogenic differentiation of human mesenchymal stem cells. *Journal of Medicinal and Nanomaterials Chemistry*, 3(2) 2021, 125-134. DOI: 10.48309/JMNC.2021.2.4